Received: 1 October 2019 | Accepted: 17 March 2020

DOI: 10.1002/hyp.13772

WILEY

A TRIBUTE TO EDWARD P. GLENN (1947-2017): A LEGACY OF SCIENTIFIC ENVIRONMENTAL ASSESSMENT AND APPLICATIONS IN HYDROLOGICAL PROCESSES

Vegetation-groundwater dynamics at a former uranium mill site following invasion of a biocontrol agent: A time series analysis of Landsat normalized difference vegetation index data

Christopher J. Jarchow[1,2] | William J. Waugh[1] | Kamel Didan[2] | Armando Barreto-Muñoz[2] | Stefanie Herrmann[3] | Pamela L. Nagler[4]

[1]Applied Studies & Technology, Navarro Research and Engineering, Inc., Grand Junction, Colorado

[2]Biosystems Engineering, University of Arizona, Tucson, Arizona

[3]School of Natural Resources and the Environment, University of Arizona, Tucson, Arizona

[4]Southwest Biological Science Center, U.S. Geological Survey, Tucson, Arizona

Correspondence
Christopher J. Jarchow, Applied Studies & Technology, Navarro Research and Engineering, Inc., 2597 Legacy Way, Grand Junction, CO 81503.
Email: chris.jarchow@lm.doe.gov, christoj@email.arizona.edu

Funding information
Department of Energy Office of Legacy Management; Desert Southwest Cooperative Ecosystem Studies Unit, Grant/Award Number: G18AC00321; National Aeronautics and Space Administration, Grant/Award Number: 80NSSC18K0617; U.S. Geological Survey

Abstract

Because groundwater recharge in dry regions is generally low, arid and semiarid environments have been considered well-suited for long-term isolation of hazardous materials (e.g., radioactive waste). In these dry regions, water lost (transpired) by plants and evaporated from the soil surface, collectively termed evapotranspiration (ET), is usually the primary discharge component in the water balance. Therefore, vegetation can potentially affect groundwater flow and contaminant transport at waste disposal sites. We studied vegetation health and ET dynamics at a Uranium Mill Tailings Radiation Control Act (UMTRCA) disposal site in Shiprock, New Mexico, where a floodplain alluvial aquifer was contaminated by mill effluent. Vegetation on the floodplain was predominantly deep-rooted, non-native tamarisk shrubs (*Tamarix* sp.). After the introduction of the tamarisk beetle (*Diorhabda* sp.) as a biocontrol agent, the health of the invasive tamarisk on the Shiprock floodplain declined. We used Landsat normalized difference vegetation index (NDVI) data to measure greenness and a remote sensing algorithm to estimate landscape-scale ET along the floodplain of the UMTRCA site in Shiprock prior to (2000–2009) and after (2010–2018) beetle establishment. Using groundwater level data collected from 2011 to 2014, we also assessed the role of ET in explaining seasonal variations in depth to water of the floodplain. Growing season scaled NDVI decreased 30% ($p < .001$), while ET decreased 26% from the pre- to post-beetle period and seasonal ET estimates were significantly correlated with groundwater levels from 2011 to 2014 ($r^2 = .71$; $p = .009$). Tamarisk greenness (a proxy for health) was significantly affected by *Diorhabda* but has partially recovered since 2012. Despite this, increased ET demand in the summer/fall period might reduce contaminant transport to the San Juan River during this period.

KEYWORDS

evapotranspiration, groundwater, Landsat, NDVI, remote sensing, tamarisk, tamarisk beetle, UMTRCA

1 | INTRODUCTION

In arid and semiarid environments, potential evapotranspiration (ET) exceeds precipitation, resulting in low to zero groundwater recharge (Wilcox, Breshears, & Seyfried, 2003). The low percolation and recharge make these areas more suitable than humid areas for long-term storage of radioactive and other hazardous waste materials (Reith & Thompson, 1992; Winograd, 1981) because leaching of contaminants into groundwater is minimized (Gee et al. (1994); Glenn, Jarchow, and Waugh (2016)). However, specific percolation rates and recharge in these environments will vary depending on local edaphic properties and vegetation conditions. Sandvig and Phillips (2006) observed deep percolation (past the root zone) in some plant communities (e.g., juniper-grass) and zero recharge in other desert communities (e.g., creosote communities), and evidence even suggests a net upward movement of water in the Desert Southwest of the United States over the past 10,000–15,000 years (Scanlon, Levitt, Reedy, Keese, & Sully, 2005). In non-vegetated conditions, deep percolation can be >50% of annual precipitation in sandy soils yet effectively be reduced in the presence of desert plants (Gee et al., 1994). In the southwestern U.S., plants have even been shown to completely eliminate deep drainage (Gee et al., 1994).

Because vegetation can help control the transport of water through the vadose zone in arid and semiarid environments, plants have been identified as a key tool for controlling the spread of contaminants into groundwater at some hazardous waste sites (Bresloff, Nguyen, Glenn, Waugh, & Nagler, 2013; DOE, 2016; Glenn et al., 2016; Jordan et al., 2008; C. A. McKeon, Jordan, Glenn, Waugh, & Nelson, 2005; C. McKeon et al., 2006). Under the Uranium Mill Tailings Radiation Control Act (UMTRCA) of 1978, the U.S. Department of Energy (DOE) Office of Legacy Management (LM) is responsible for managing stored hazardous and radioactive waste at former uranium ore processing sites throughout the United States, including sites in the Desert Southwest. As such, LM monitors and manages groundwater where contamination exceeds regulatory standards in Title 40 *Code of Federal Regulations* Section 192.20. At uranium disposal sites on Navajo land (the Four Corners region of the United States), researchers are evaluating vegetation to hydraulically control groundwater contamination plumes (Waugh, Glenn, Charley, Maxwell, & O'Neill, 2011). Studies at these sites have shown that annual ET of deep-rooted plant communities is capable of exceeding annual precipitation, thereby limiting the leaching of contaminants into shallow aquifers. However, land disturbances such as grazing can limit ET in these areas, potentially leading to groundwater recharge and mobilization of groundwater contaminants (Bresloff et al., 2013; Glenn et al., 2016).

Because ET is an important tool for the management of contaminants at uranium mill tailings sites in the Desert Southwest, assessment of this parameter is crucial to long-term monitoring activities. Our study consisted of two parts. First, we used satellite remote sensing techniques to assess ET-groundwater dynamics of an UMTRCA site in Shiprock, New Mexico, where ammonium, manganese, nitrate, selenium, strontium, sulphate, and uranium were identified as contaminants of concern (DOE, 2002). A study conducted from 2011 to 2014 found that groundwater levels at this site were lower in the late summer/fall than in the winter/early spring, despite similar gage elevations on the adjacent San Juan River (DOE, 2018). Evapotranspiration was proposed as the likely cause of the river-groundwater elevation differences. The authors suggested that ET could act as a natural form of remediation pumping, preventing or minimizing the spread of the contaminant plume into the river during the late summer/fall period. We used a regionally calibrated ET remote sensing algorithm to determine if spatially and temporally explicit estimates of ET could explain the groundwater-river level dynamics in this system.

The floodplain of the Shiprock UMTRCA site is dominated by a large stand of non-native tamarisk (*Tamarix* sp.) shrubs and trees; this phreatophyte (deep-rooted plants capable of accessing shallow groundwater) has replaced many native riparian plant communities in the western U.S. (Glenn & Nagler, 2005). In an effort to control tamarisk spread, the tamarisk beetle (*Diorhabda* spp.) was introduced to the western U.S. as a biological control agent. By defoliating tamarisk over multiple generations, the beetle can kill the plants by stopping photosynthesis. Since its initial release in 2001, the beetle has expanded significantly in the southwestern U.S., leading to widespread defoliation of tamarisk (Dennison, Nagler, Hultine, Glenn, & Ehleringer, 2009; Dudley & Bean, 2012; Jamison, van Riper, & Bean, 2015; Meng et al., 2012). A large release of beetles in 2007 on the San Juan River in Bluff, Utah, was about 100 km downgradient of the Shiprock site. The beetle was first observed at multiple locations near the Shiprock site from 2010 to 2014 (Rivers Edge West, 2018) and has since defoliated the majority of tamarisk on the floodplain (Waugh, personal obs.). Defoliation of tamarisk, the dominant riparian species on the Shiprock floodplain, could affect the groundwater contaminant plume described in DOE (2018). The second part of our study was a long-term analysis of ET and vegetation greenness using Landsat 5, 7 and 8 imagery to determine if, and to what extent, ET has been affected by changes in tamarisk health prior to (2000–2009) and after (2010–2018) beetle arrival.

2 | METHODS

2.1 | Study site and relevant history

Our study area included the San Juan River floodplain adjacent to the UMTRCA disposal site in Shiprock, New Mexico, United States (Figure 1). This area of northwestern New Mexico is arid, with an average annual rainfall of 179 mm and 99 mm of snowfall. Temperatures range from average winter lows of −6°C to mean summer highs of 32°C. Although this area is dry, the perennial San Juan River bordering the site supports a lush riparian ecosystem. Soil on the floodplain is predominantly stream alluvium (Bebeevar-Walrees complex; Natural Resources Conservation Service (NRCS) (n.d.)). The water table was shallow, with an average depth of 2.03 m in the winter/spring and 2.06 m in the summer/fall in the area defined as the unpumped zone (described below; DOE (2018)). Vegetation along the

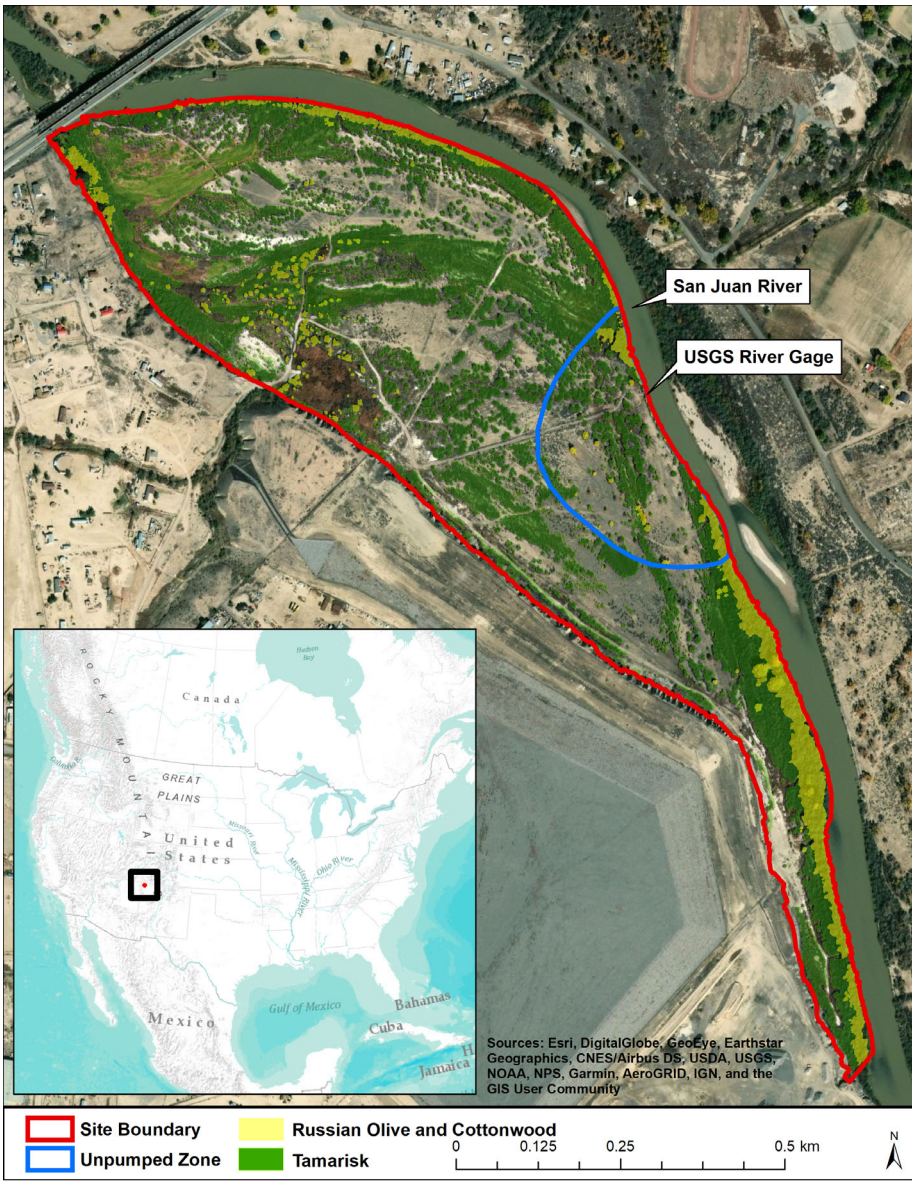

FIGURE 1 Floodplain of the Shiprock, New Mexico Uranium Mill Tailings Radiation Control Act (UMTRCA) site. The unpumped zone is an approximate boundary

floodplain was primarily composed of phreatophytes and included tamarisk, Russian olive (*Elaeagnus angustifolia*), willow (*Salix* sp.), Freemont cottonwood (*Populus fremontii*), Siberian elm (*Ulmus pumila*), fourwing saltbush (*Atriplex canescens*), black greasewood (*Sarcobatus vermiculatus*), and rubber rabbitbrush (*Ericameria nauseosa*). See Luttge and Beyschlag (2014) and Robinson (1958) for a full description of rooting and other characteristics of these species. Dominant understory forbs and grasses were kochia (*Bassia scoparia*), Russian thistle (*Salsola tragus*), saltgrass (*Distichlis spicata*) and Indian ricegrass (*Achnatherum hymenoide*). The growing period in this area is typically June–September and was defined in this study as June 1–September 30.

The Shiprock mill operated from 1954 to 1968, but infiltration of contaminants likely continued for more than 30 years from mill startup to completion of surface remediation in 1986 (DOE, 2018). A floodplain remediation system consisting of natural flushing and pumping wells to extract groundwater was implemented by the DOE in 2003. The objective of pumping was to reduce discharge to the San Juan River and reduce contaminant levels to the point where natural flushing would be the primary remediation method. Remediation pumping in these wells intentionally altered surrounding groundwater flow patterns, except for one area identified in DOE (2018) as unaffected by pumping activities (Figure 1).

2.2 | Delineation of study and control sites

To assess long-term tamarisk health, we first digitized all tamarisk (ca. 21 ha) existing on the floodplain using high-resolution (9 cm) unmanned aerial system (UAS), or drone, imagery acquired by the U.S. Geological Survey (USGS) in the summer of 2016 (Figure 1). At this resolution, we easily identified and separated live, dead, or defoliated tamarisk from other species at the site. Although tamarisk beetles arrived around 2010, high-resolution satellite imagery from

2004 confirmed that the distribution of tamarisk at the site had not changed since that time; therefore, we only used one mask to assess tamarisk condition from 2000 to 2018. We then delineated a zone (ca. 4 ha) corresponding to two other significant phreatophytic species on the floodplain (Russian olive and cottonwood), which were identifiable in the U.S. aerial image by their distinctive colour and texture. To assess the effect of ET on groundwater levels in the floodplain, we digitized a third mask (ca. 6 ha) corresponding to an area of the floodplain identified in DOE (2018) as unaffected by remediation pumping and referred to here as the unpumped zone (Figure 1).

2.3 | Data acquisition

We obtained all available atmospherically corrected Landsat Collection 1 Tier 1 normalized difference vegetation index (NDVI) images (WRS path 035 and row 035) using the USGS Earth Resources Observation and Science Center Science Processing Architecture On Demand Interface (https://espa.cr.usgs.gov/). The data set included NDVI images from three consecutive Landsat sensors: Landsat 5 Thematic Mapper (TM; 2000–2011), Landsat 7 Enhanced Thematic Mapper Plus (ETM+; 2012), and Landsat 8 Operational Land Imager (OLI; 2013–2018). The NDVI is a numerical indicator of the presence and health of green vegetation calculated from the near-infrared (NIR) and red (R) portions of reflected electromagnetic radiation according to Equation (1):

$$(\mathrm{NIR}-\mathrm{R})/(\mathrm{NIR}+\mathrm{R}) \quad (1)$$

The Landsat 7 ETM+ period (2012) represents the year between the decommissioning of Landsat 5 and the launch of Landsat 8. Because of the Scan Line Corrector failure on Landsat 7 in 2003, images collected after this period contained streaks of missing data, precluding application of this platform in some areas; however, the majority of our site fell between these streaks of missing pixels, allowing us to use ETM+ for 2012.

To eliminate spurious data that may impact ET estimates, we implemented a per-pixel quality assurance screening that eliminated all pixels flagged as clouds or shadows. To further minimize the impact of adjacent clouds and cloud shadow, we also removed an 8-pixel-wide buffer around all cloudy pixels. Only data that passed this strict filtering method were retained for further analysis. This process resulted in four to seven images per growing season, with a total of 112 scenes from 2000 to 2018 (Table 1).

To compare tamarisk health to discharge of the neighbouring San Juan River, we obtained daily river discharge data from the USGS for 2000–2018 (station 09368000; Figure 1). We calculated mean river discharge for May 1–September 30. We defined the growing period from June 1–September 30 based on an 18-year average of 16-day NDVI from the Moderate Resolution Imaging Spectroradiometer, but included May in the calculation of mean river discharge to account for any potential lag response following spring snowmelt (increased discharge), which typically occurs from May to June (DOE, 2018).

TABLE 1 Mean growing season scaled NDVI (NDVI*) for the tamarisk and unpumped zones (2000–2018)

Sensor	Year	Number of scenes	NDVI* tamarisk zone	NDVI* unpumped zone
TM	2000	4	0.2747	0.1427
TM	2001	5	0.3061	0.1704
TM	2002	7	0.2392	0.1418
TM	2003	7	0.2786	0.1587
TM	2004	7	0.2890	0.1682
TM	2005	7	0.3566	0.2282
TM	2006	7	0.2765	0.1663
TM	2007	4	0.3161	0.1817
TM	2008	6	0.3440	0.2064
TM	2009	4	0.3048	0.1699
TM	2010	6	0.2037	0.1288
TM	2011	4	0.1869	0.1081
ETM+	2012	6	0.1660	0.0928
OLI	2013	7	0.1765	0.1256
OLI	2014	7	0.1923	0.1162
OLI	2015	4	0.2591	0.1555
OLI	2016	7	0.2218	0.1389
OLI	2017	7	0.2874	0.1767
OLI	2018	6	0.1827	0.1255

Abbreviations: ETM, Enhanced Thematic Mapper; NDVI, normalized difference vegetation index; OLI, Operational Land Imager.

Reliable precipitation data were not available for Shiprock, so we obtained annual precipitation for 2000–2018 from the Four Corners Regional Airport in Farmington, New Mexico (station USW00023090) approximately 40 km east of our study site.

2.4 | NDVI scaling and estimation of ET

The Landsat TM, ETM+ and OLI sensors have slightly different dynamic ranges and scales, which leads to interscene variability that can potentially complicate the ET and NDVI analysis. Residual atmosphere, sun and viewing geometry and soil/vegetation composition (Huete & Liu, 1994; Liu & Huete, 1995) can introduce additional variability. To minimize this scene-to-scene variability and allow cross-sensor comparisons through time, we scaled NDVI values (NDVI*; Equation 2) between bare soil ($NDVI_0$) and maximum vegetation (saturation; $NDVI_s$) following Groeneveld and Baugh (2007). This scaling process stretches values between baseline soil (low NDVI) and maximum NDVI within each scene, thereby standardizing values between time periods and removing variability due to atmospheric, soil and other factors. We sampled a constant area of bare soil in each scene to derive mean $NDVI_0$, while we calculated $NDVI_s$ by taking the average of all pixels falling within 5% of the maximum value for all irrigated, verdant agricultural fields identifiable in each image (Jarchow, Nagler, & Glenn, 2017):

$$NDVI* = (NDVI - NDVI_0)/(NDVI_s - NDVI_0) \quad (2)$$

Because this stretching process relies on saturated values of NDVI, we only used scenes acquired during the growing season (generally from June to September). We subsequently obtained peak and mean growing season (June 1–September 30) NDVI* for the tamarisk and unpumped zones.

We used a remote sensing algorithm developed by Groeneveld, Baugh, Sanderson, and Cooper (2007) to estimate long-term (2000–2018) annual ET along the Shiprock floodplain. The algorithm was derived from the empirical relationship between Landsat NDVI data and ET measured by eddy covariance or Bowen ratio method for phreatophytic plants in three different regions of the arid southwestern U.S. (Groeneveld et al., 2007). Vegetation communities used to calibrate the algorithm were very similar to those found on our study site, including tamarisk, cottonwood, greasewood and rabbitbrush.

Normalized difference vegetation index leverages differences in absorbance in the red and NIR wavelengths of light. Chlorophyll, the pigment responsible for green coloration in plants, absorbs most blue and red light, while the surrounding plant tissues reflect in the NIR (Buschmann & Nagel, 1993). Because chlorophyll is the primary pigment responsible for absorbing the light that drives photosynthesis, the rate of photosynthesis is directly related to the amount of chlorophyll present (Sellers, Berry, Collatz, Field, & Hall, 1992; Tucker & Sellers, 1986). Therefore, NDVI responds to actively photosynthesizing material, increasing as the quantity of green biomass increases (Burgan & Hartford, 1993). Since photosynthesis requires leaf conductance for uptake of carbon dioxide, water is lost during this process through transpiration. As a result, NDVI can be used as a competent predictor of ET (Glenn et al., 2016; Groeneveld et al., 2007; Jarchow et al., 2017; Kerr et al., 1989).

We used a modified version of the algorithm developed by Groeneveld et al. (2007) to estimate ET:

$$ET = ET_o(NDVI*) \quad (3)$$

where ET is annual estimated evapotranspiration, ET_o is annual reference crop evapotranspiration as determined by the Blaney-Criddle (BC) equation (Brouwer & Heibloem, 1986), and NDVI* is scaled peak season NDVI. Peak NDVI was obtained by finding the scene with the highest average NDVI* for each year. Equation (3) originally included the component of annual precipitation, but we removed this to estimate groundwater discharge in this predominantly phreatophytic system (Glenn et al., 2016; Jarchow et al., 2017). Reference crop ET was calculated for 2000–2018 using meteorological data from the Four Corners Regional Airport (2000–2004) in Farmington, New Mexico, and a remote weather station at the disposal site (2005–2018). Complete meteorological data for 2000–2004 were neither available for the site nor the town of Shiprock, so data from Farmington were used instead. Values from Equation (3) provided an estimate of annual ET.

For the tamarisk zone, we calculated mean growing period NDVI* and annual ET for all years (2000–2018). As mentioned previously, DOE (2018) analysed groundwater levels of three monitoring wells on the floodplain that were unaffected by remediation pumping. Because we were interested in the seasonal relationship between ET and groundwater elevation in the unpumped zone, we compared ET to roughly the same periods reported in DOE (2018)(winter/spring and summer/fall). The exact dates used to derive mean groundwater elevation in DOE (2018) differed between years because they were chosen to avoid large changes in groundwater level caused by substantial, long-lasting changes in river flow. To account for potential lag time between changes in ET and groundwater elevation, we standardized the winter/spring and summer/fall periods for ET estimation (i.e., January 1–May 31 and June 1–October 31, respectively). While the Groeneveld et al. (2007) method of ET estimation produced annual values, we also estimated seasonal ET assuming a proportional relationship between ET and ET_o, for which seasonal values were known. We assumed seasonal ET would generally track ET_o because shallow groundwater was not a limiting factor (Nichols et al., 2004).

2.5 | Statistical analyses

We used multiple linear regression to assess the relationship between mean growing season NDVI* and the predictor variables (annual precipitation and mean river discharge). We tested the predictor variables for collinearity following Dormann et al. (2013), where an absolute correlation coefficient (r) rejection threshold of >.70 between predictor variables was applied. To assess the strength of association between individual variables, we used Pearson's correlation

coefficient (r). For the unpumped zone, we log-transformed groundwater elevations and seasonal estimates of ET. A paired t-test was used to determine the significance of change in NDVI* prior to (2000–2009) and following (2010–2018) establishment of tamarisk beetles near the site.

3 | RESULTS AND DISCUSSION

3.1 | Tamarisk zone

Mean growing season NDVI* of tamarisk varied from year to year, with a low of 0.1660 in 2012 and a high of 0.3566 in 2005 (Figure 2; Table 1). Peak NDVI* showed a similar trend, with a low of 0.1958 in 2012 and a high of 0.4262 in 2005 (Table 2). Growing season NDVI* decreased 30% from 2000–2009 to 2010–2018, with a mean of 0.2985 and 0.2085 for these periods, respectively (difference = 0.0901; $p < .001$). During the same periods, ET decreased 26% from a mean annual total of 484–359 mm (Figure 3). As with NDVI*, 2005 had the highest total annual ET (618 mm), while 2012 had the lowest (286 mm).

The reduction in ET from 2000–2009 to 2010–2018 was slightly higher than that reported by Nagler et al. (2018), who observed a 21% decrease on the San Juan at Shiprock following arrival of the beetle; however, the lower estimate they reported was likely due to a different definition of the pre- and post-beetle infestation period (they defined 2007 the initial year of infestation). As discussed previously, the tamarisk beetle was first observed near the Shiprock site in 2010 (Rivers Edge West, 2018); however, our data showed a rapid decline in NDVI* starting in 2009 that continued through 2012 (Figure 2). The beetle was also observed in 2008 and 2009 on the Mancos River in southern Colorado at approximately the same distance to our site from the introduction site in Bluff, Utah. Nagler et al. (2018) also observed a 2-year lag between introduction of the beetle (2007) and resulting decrease in tamarisk greenness near our site in Shiprock. Based on the above evidence, the beetle was likely established on the Shiprock floodplain by 2009.

Because tamarisk is phreatophytic and depth to groundwater at our study site tended to be low, we expected NDVI* to closely track river discharge. We found that the highest mean river discharge occurred in 2005 (98.95 $m^3\ s^{-1}$), while the lowest (16.52 $m^3\ s^{-1}$) was observed in 2002 (Figure 2). While years of peak NDVI* and discharge corresponded (i.e., 2005), the years in which minimum values were observed differed (2012 and 2002, respectively). Based on multiple regression analysis, mean river discharge was significantly correlated with mean growing season NDVI* from 2000 to 2018 ($p = .002$), but precipitation was not a significant predictor of NDVI* during this period ($p = .92$); however, the overall predictive power of the model was weak ($r^2 = .46$). Additionally, precipitation and mean river discharge were not correlated ($r^2 = .05$; $p = .34$). Despite the weak predictive power of the model for the 19-year study period, mean growing season NDVI* was highly correlated with river discharge ($r^2 = .92$) during the pre-beetle period (2000–2009), but was only weakly correlated during the post-beetle period of 2010–2018 ($r^2 = .67$). The latter finding is significant because it supports the idea that prior to beetle arrival, tamarisk greenness (and thus ET) was primarily driven by river flows. Additionally, growing season NDVI* was not correlated with annual precipitation for the pre-beetle, post-beetle or whole period of record (Table 3), further supporting the role of river flows and effect of beetles on tamarisk at the disposal site. This is also supported by the difference in years corresponding to minimum discharge and NDVI*. Prior to beetle arrival, both maximum and minimum river discharge and NDVI* occurred in the same years (2005 and 2002, respectively).

From 2008 to 2012, NDVI* steadily declined to its lowest level in 2012 before slightly increasing in 2013. The decline in NDVI* post-beetle arrival is further complicated by a decrease in mean river discharge during the same period, with a mean of 54.11 from 2000 to 2009 and 45.51 $m^3\ s^{-1}$ from 2010 to 2018; however, this 16% reduction in discharge is disproportionately less than would be expected based on the reduction of ET and NDVI* observed during the same period. Further, NDVI* of two species unaffected by the beetle (Russian olive and cottonwood) did not change significantly from the pre- to post-beetle period ($mean_{2000–2009}$ = 0.4942;

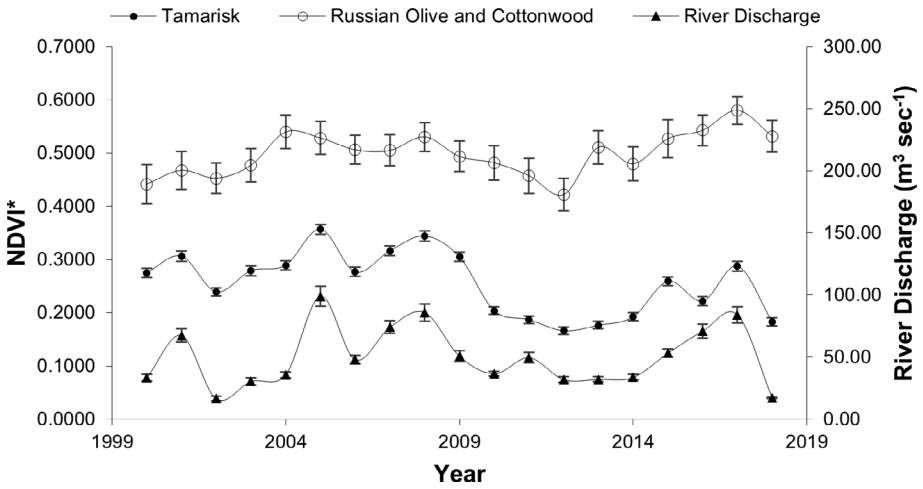

FIGURE 2 Mean growing season scaled normalized difference vegetation index (NDVI*) and mean river discharge for all years analysed. Bars are *SE*

TABLE 2 Landsat 5 Thematic Mapper (TM), Landsat 7 Enhanced Thematic Mapper Plus (ETM+), and Landsat 8 Operational Land Imager (OLI) overpass dates and associated NDVI values and scaling parameters corresponding to the period of peak greenness

Sensor	Overpass date	$NDVI_0$	$NDVI_s$	Peak $NDVI_{Raw}$ (tamarisk zone)	NDVI* (tamarisk zone)	Peak $NDVI_{Raw}$ (unpumped zone)	NDVI* (unpumped zone)
TM	July 18, 2000	0.0821	0.8720	0.3325	0.3170	0.2086	0.1607
TM	September 7, 2001	0.0776	0.8583	0.3546	0.3548	NA	NA
TM	September 23, 2001	0.0794	0.8585	NA	NA	0.2347	0.2006
TM	July 24, 2002	0.0717	0.8621	0.2889	0.2749	0.1932	0.1550
TM	September 13, 2003	0.0752	0.8736	0.3139	0.2990	0.2235	0.1857
TM	July 29, 2004	0.0809	0.8696	0.3372	0.3250	0.2275	0.1859
TM	August 17, 2005	0.0864	0.8826	0.4258	0.4262	0.3087	0.2792
TM	July 19, 2006	0.0766	0.8546	0.3175	0.3097	0.2138	0.1770
TM	August 23, 2007	0.0709	0.8618	0.3362	0.3355	0.2205	0.1904
TM	August 9, 2008	0.0943	0.8721	0.4078	0.4030	0.2810	0.2400
TM	July 27, 2009	0.0988	0.8710	0.3636	0.3430	0.2444	0.1895
TM	July 30, 2010	0.1060	0.8795	0.3184	0.2746	0.2346	0.1663
TM	September 19, 2011	0.0949	0.8764	0.2748	0.2302	0.2005	0.1352
ETM+	June 9, 2012	0.0721	0.8679	0.2279	0.1958	NA	NA
ETM+	July 11, 2012	0.0691	0.8888	NA	NA	0.1755	0.1298
OLI	September 24, 2013	0.0970	0.9430	0.3086	0.2500	0.2749	0.2102
OLI	July 9, 2014	0.0969	0.9517	0.3004	0.2384	0.2228	0.1488
OLI	August 13, 2015	0.1385	0.9609	NA	NA	0.2741	0.1650
OLI	June 26, 2015	0.1420	0.9117	0.3479	0.2681	NA	NA
OLI	September 16, 2016	0.1148	0.9084	0.3308	0.2722	0.2454	0.1667
OLI	August 18, 2017	0.1127	0.9622	0.3722	0.3054	0.2680	0.1836
OLI	June 18, 2018	0.0923	0.9090	0.2610	0.2066	0.2150	0.1501

Note: $NDVI_s$ (saturation) and $NDVI_0$ (bare soil) were used to calculate scaled NDVI (NDVI*).

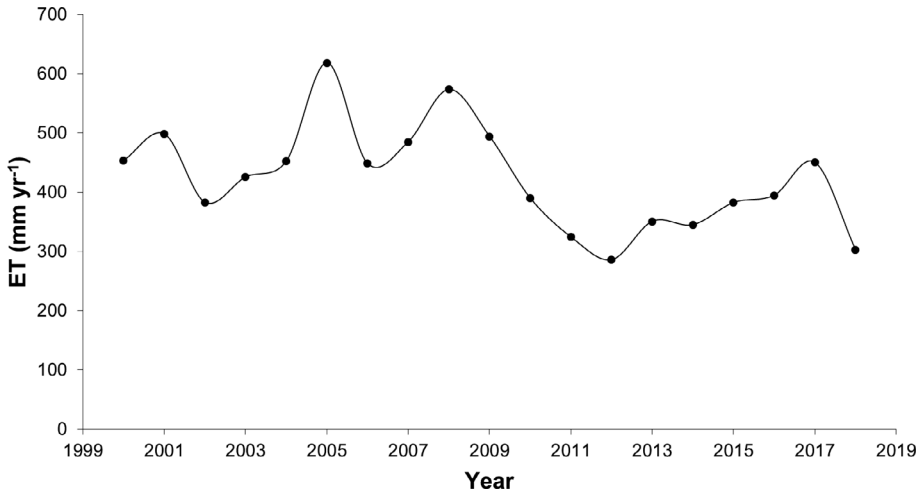

FIGURE 3 Annual evapotranspiration (ET) of tamarisk on the Shiprock floodplain for all years analysed

TABLE 3 Regression analysis of mean growing season scaled NDVI (NDVI*) and annual precipitation for the whole period of record (2000–2018), pre-beetle period (2000–2009), and post-beetle period (2010–2018)

Period	r^2	*p*-Value	Lower 95%	Upper 95%
2000–2018	.02	.57	−0.0005	0.0008
2000–2009	.02	.72	−0.0007	0.0009
2010–2018	.20	.23	−0.0003	0.0009

$mean_{2010–2018}$ = 0.5037; p = .298; Figure 2). It is likely that reduced river flows combined with defoliation by beetles both contributed to the substantial decline in tamarisk health after 2009, but our findings in the Russian olive and cottonwood zone suggest the beetle was the primary driver of this decline.

3.2 | Unpumped zone

DOE (2018) compared groundwater elevations across the floodplain to river elevations reported at the USGS river gage (Figure 1) for the years 2006–2011. River elevations in the spring and fall were within ~120 mm in 5 of the 6 years sampled, while mean floodplain-wide groundwater levels were ~300–600 mm lower in the fall than in the spring. Because the authors' floodplain-wide analysis was potentially affected by remediation pumping activities in certain areas, they conducted a follow-up analysis of wells from 2011 to 2014 identified as unaffected by remediation pumping (unpumped zone; Figure 1). Two key findings were reported: (a) Groundwater in the unpumped zone was lower in the summer/fall than the spring/winter, despite relatively stable river elevations. This was particularly true of wells located farther from the river, which were less affected by short-term changes in river stage; and (b) the river loses water to the alluvial aquifer during the late summer/fall and groundwater mostly discharges to the river in the winter/spring. Lacking evidence supporting alternative causes, the authors postulated that discharge via ET of alluvial groundwater was the most likely cause of the summer/fall river losses. The latter is significant because changes in flow direction associated with spatially variable ET could help explain apparent lateral spreading of uranium and sulphate plumes in this system DOE (2018).

To investigate the possible role of ET in decreasing groundwater levels, we focused our ET analysis on the unpumped zone for the periods for which groundwater data were reported in DOE (2018) (winter/spring and summer/fall of 2011–2014; Table 4). Winter/spring and summer/fall groundwater levels from 2011–2014 were significantly correlated with ET (r^2 = .71; p = .009; Figure 4). Mean ET during the winter/spring for 2011–2014 was 76 mm, compared to 127 mm in the summer/fall (Table 5). DOE (2018) reported only minor differences in groundwater elevations between the winter/spring and summer/fall periods in 2013, which they attributed to higher-than-average river flow during the late summer. In support of their conclusion, we observed the greatest increase in ET from the winter/spring to summer/fall in 2013 (Table 5) and a 35% increase in growing season NDVI* in the unpumped zone versus only a 6% increase in the tamarisk zone (Figure 5).

TABLE 4 Mean groundwater (well) level (elevation) above mean sea level by season and corresponding evapotranspiration (ET) estimates for years 2011–2014

Year	Season	Mean well water level (m)	Total ET (mm)
2011	Winter/ Spring	1,488.71	64
2012	Winter/ Spring	1,488.61	66
2013	Winter/ Spring	1,488.53	100
2014	Winter/ Spring	1,488.56	74
2011	Summer/Fall	1,488.49	110
2012	Summer/Fall	1,488.47	107
2013	Summer/Fall	1,488.48	170
2014	Summer/Fall	1,488.48	122

Note: Mean water level was calculated from values reported in DOE (2018). Mean surface elevation was ~1,490 m.

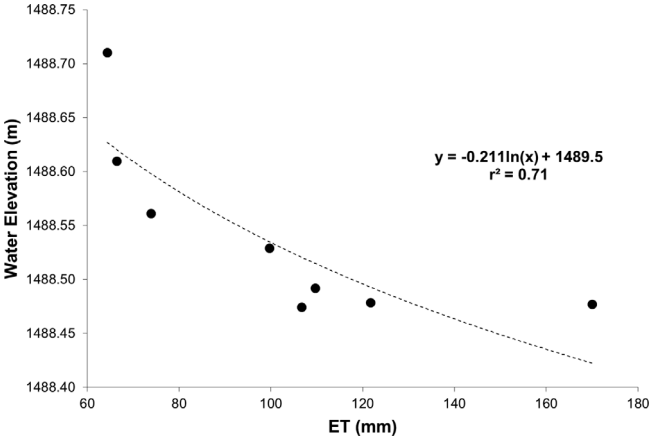

FIGURE 4 Groundwater elevation (level) versus evapotranspiration (ET) of the unpumped zone during the winter/spring and summer/fall periods (2011–2014)

3.3 | Tamarisk recovery

As discussed previously, tamarisk NDVI* reached its lowest point in 2012, followed by a steady increase through 2017. During this period, greenness generally tracked river flow (Figure 2), except in 2016. NDVI* was lower in 2016 than in 2015 and 2017, while mean river discharge increased from 2015 to 2017. Between-year fluctuations in abundance have been observed in *Diorhabda* following large defoliation events, which is likely driven by resource depletion (Jamison et al., 2015; Kennard et al., 2016). Jamison, Johnson, Bean, and van

Riper (2018) found that beetle larvae were less likely to establish in areas where defoliation exceeded 70%, leading to a temporary loss of beetles and refoliation of tamarisk. The anomalous dip in NDVI* we observed in 2016 could represent a second, brief beetle defoliation event. This explanation is also supported by our findings in the Russian olive and cottonwood zone, where NDVI* increased from 2015 to 2016 (Figure 2). A substantial decrease in NDVI* was also observed in 2018, but this coincided with the lowest river discharge and precipitation recorded during the entire period of study. Years 2015–2018 could also represent an annual refoliation-defoliation-refoliation cycle, with 2018 being exacerbated by low river flows.

Despite the dips in NDVI* observed in 2016 and 2018, 2013 marked the end of a 4-year decline in greenness following the establishment of the beetle. Nagler et al. (2018) reported a similar trend for 2004–2016 for the San Juan River at Shiprock using the enhanced vegetation index, another measure of plant greenness, and noted a cycle of beetle colonization-defoliation-emigration, followed by a period of plant recovery. Consistent with our results, they also observed a 4–5-year decline in tamarisk health following beetle colonization before beginning a period of recovery. Despite this recovery, average peak NDVI* in the current study was 24% lower during the recovery period (2013–2018) than the pre-infestation period (2000–2008). Decreased river discharge during the post-infestation period may have had a role in the reduction of NDVI*, but NDVI values of nearby Russian olive and cottonwood did not change significantly during these periods.

Although we used high-resolution aerial imagery to digitize the tamarisk zone, we cannot eliminate the possibility that other vegetation may have established under the tamarisk canopy, especially following defoliation events. During a ground survey conducted in October 2018, we observed a mosaic of completely defoliated, partially defoliated, and refoliated tamarisk, but very few plants were observed to be established directly under the tamarisk canopy. Where plants did exist under or near tamarisk, it was limited mostly to small annuals associated with young (mostly unbranched), small tamarisk shrubs; therefore, we do not suspect other plants contributed significantly to NDVI*.

TABLE 5 Evapotranspiration (ET) of the unpumped zone during the winter/spring and summer/fall periods for years 2011–2014

Year	Winter/Spring ET	Summer/Fall ET	Difference
2011	64	110	46
2012	66	107	41
2013	100	170	70
2014	74	122	48
Mean	76	127	51

Note: Values are in mm.

3.4 | Error in ET estimates

Validation data were not available to quantify the error in our remote sensing ET estimates, but Groeneveld et al. (2007) reported mean errors ranging from 2.0 to 12.5% in vegetation communities similar to that in the current study. One difference in our application of this technique was the use of Blaney-Criddle ET_o instead of Penman-Monteith (PM; Allen, Pereira, Raes, & Smith, 1998). Penman-Monteith is recommended over other methods because it is physically based and explicitly incorporates physiological and aerodynamic data, but it requires a large number of climatic parameters. Such input data were not available for Shiprock. Blaney-Criddle is a simpler technique, only requiring a direct measurement of temperature. In arid environments, differences between PM and BC may range from <1% to >30%, with BC commonly overestimating ET_o with respect to PM (Tabari, Hosseinzadeh Talaee, & Some'e, 2013).

As an independent check of our ET estimates, we estimated the specific yield of the alluvial aquifer using our ET estimates and the groundwater measurements reported for 2011 and 2012. We chose these years because the groundwater sampling periods most closely matched our winter/spring and summer/fall ET periods, and river

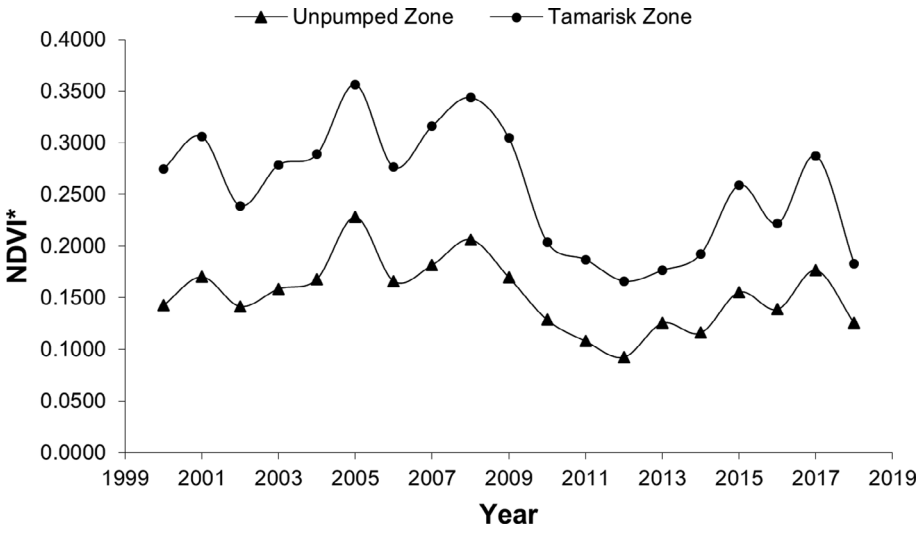

FIGURE 5 Scaled NDVI (NDVI*) of the tamarisk and unpumped zones for all years analysed. NDVI, normalized difference vegetation index

stage was most stable in 2011 and 2012 following spring snowmelt. We estimated a mean specific yield of 26% across years, compared to 25% reported for the floodplain alluvial aquifer in DOE (2018)—in good agreement with our estimate. Similarly, Glenn et al. (2016) constructed a water balance at a UMTRCA site in Tuba City, Arizona using the same ET estimation method, and they found that measured gain in a nearby stream was within 15% of the value predicted by their ET model. These indirect assessments suggest reasonably high accuracy using the Groeneveld et al. (2007) method coupled with BC ET_o.

3.5 | Management implications

From 2000 to 2009, average annual ET within the tamarisk zone was 99,749 m^3, but it decreased to 73,911 m^3 from 2010 to 2018––a loss of 25,838 m^3. Even during the period of lowest NDVI* and ET (2011–2014), groundwater levels in the summer/fall were still lower than in the winter/spring, resulting in river losses to the aquifer (DOE, 2018). During this same period, we estimated mean ET was 67% higher in the unpumped zone in the summer/fall than in the winter/spring, supporting the findings in DOE (2018). Therefore, river losses to the aquifer via ET from 2011 to 2014 likely represent a conservative estimate, especially considering the recovery of tamarisk we observed since 2014 (Figure 2). These findings indicate that temporally and spatially explicit ET estimates should be considered as part of an overall groundwater remediation strategy, as resource management practices (e.g., introduction of biocontrol agents) can affect ET rates across time and space. Spatial estimates of ET could be used in conjunction with groundwater data to help inform the future placement of groundwater extraction wells.

4 | CONCLUSIONS

This study demonstrated the long-term effect of tamarisk beetles on tamarisk health and the potential effect of ET on local groundwater dynamics at a former uranium mill site in Shiprock, New Mexico. We found that the tamarisk beetle likely had a significant effect on NDVI* and ET of tamarisk, effectively reducing the volume of ET discharged from the shallow alluvial aquifer. Based on our results, ET likely explains the reduced groundwater levels observed in the summer/fall, which could affect contaminant transport and concentrations in the alluvial groundwater. However, the substantial reduction in tamarisk health following arrival of the beetle in 2009 means the potential effect of ET on groundwater dynamics for years 2011–2014 was likely reduced compared to the pre-beetle colonization period. The latter is important because tamarisk is currently the dominant phreatophytic species on the floodplain and has replaced many native riparian plant communities in the southwestern U.S. Because tamarisk health will vary across space (characteristic of the beetle colonization-defoliation-emigration cycle) and ET may affect the spatial dynamics of contaminant transport and contaminant concentrations, spatially explicit ET estimates should be incorporated into efforts to model and remediate contaminated groundwater in such environments.

ACKNOWLEDGEMENTS

This research is dedicated to the late Dr Edward Glenn, whose ideas inspired the development and pursuit of this study. Funding was provided by the U.S. Department of Energy (DOE) Office of Legacy Management, the U.S. Geological Survey (USGS), Desert Southwest Cooperative Ecosystem Studies Unit agreement #G18AC00321 (P.I. Kamel Didan), and the National Aeronautics and Space Administration agreement #80NSSC18K0617 (P.I. Kamel Didan). We wish to thank John Vogel and Geoffrey Debenedetto from the U.S. Department of the Interior Office of Aviation Services for providing the unmanned aircraft system (UAS) flights and processing the data as part of an award to the USGS and DOE through the first UAS research program (2015). We also thank the two anonymous reviewers who helped improve this manuscript. Any use of trade, product, or firm names is for descriptive purposes only and does not imply endorsement by the U.S. Government.

DATA AVAILABILITY STATEMENT

The data that support the findings of this study are available from the corresponding author upon reasonable request.

ORCID

Christopher J. Jarchow https://orcid.org/0000-0002-0424-4104

REFERENCES

Allen, R. G., Pereira, L. S., Raes, D., & Smith, M. (1998). Crop evapotranspiration—Guidelines for computing crop water requirements. *FAO Irrigation and drainage paper 56*. Rome, Italy.

Bresloff, C. J., Nguyen, U., Glenn, E. P., Waugh, J., & Nagler, P. L. (2013). Effects of grazing on leaf area index, fractional cover and evapotranspiration by a desert phreatophyte community at a former uranium mill site on the Colorado Plateau. *Journal of Environmental Management*, *114*, 92–104. https://doi.org/10.1016/j.jenvman.2012.09.026

Brouwer, C., & Heibloem, M. (1986). Irrigation water management. FAO Corporate Repository.

Burgan, R. E., & Hartford, R. A. (1993). Monitoring vegetation greenness with satellite data. *General Technical Reports*. Ogden, UT: U. S. Department of Agriculture, Forest Service, Intermountain Research Station.

Buschmann, C., & Nagel, E. (1993). In vivo spectroscopy and internal optics of leaves as basis for remote sensing of vegetation. *International Journal of Remote Sensing*, *14*(4), 711–722. https://doi.org/10.1080/01431169308904370

Dennison, P. E., Nagler, P. L., Hultine, K. R., Glenn, E. P., & Ehleringer, J. R. (2009). Remote monitoring of tamarisk defoliation and evapotranspiration following saltcedar leaf beetle attack. *Remote Sensing of Environment*, *113*(7), 1462–1472. https://doi.org/10.1016/j.rse.2008.05.022

DOE, U. S. Department of Energy. (2002). Final ground water compliance action plan for remediation at the Shiprock, New Mexico, UMTRCA site. Grand Junction, CO.

DOE, U. S. Department of Energy. (2016). Monitored natural and enhanced attenuation of the alluvial aquifer and subpile soils at the Monument Valley, Arizona, Processing Site: Final Pilot Study Report. Grand Junction, CO.

DOE, U. S. Department of Energy. (2018). Flow processes in the floodplain alluvial aquifer at the Shiprock, New Mexico, disposal site. Washington, DC.

Dormann, C. F., Elith, J., Bacher, S., Buchmann, C., Carl, G., Carré, G., … Lautenbach, S. (2013). Collinearity: A review of methods to deal with it and a simulation study evaluating their performance. *Ecography*, *36*(1), 27–46. https://doi.org/10.1111/j.1600-0587.2012.07348.x

Dudley, T. L., & Bean, D. W. (2012). Tamarisk biocontrol, endangered species risk and resolution of conflict through riparian restoration. *BioControl*, *57*(2), 331–347. https://doi.org/10.1007/s10526-011-9436-9

Gee, G. W., Wierenga, P. J., Andraski, B. J., Young, M. H., Fayer, M. J., & Rockhold, M. L. (1994). Variations in water balance and recharge potential at three Western Desert sites. *Soil Science Society of America*, *58*, 63–72.

Glenn, E. P., Jarchow, C. J., & Waugh, W. J. (2016). Evapotranspiration dynamics and effects on groundwater recharge and discharge at an arid waste disposal site. *Journal of Arid Environments*, *133*, 1–9. https://doi.org/10.1016/j.jaridenv.2016.05.003

Glenn, E. P., & Nagler, P. L. (2005). Comparative ecophysiology of *Tamarix ramosissima* and native trees in western U.S. riparian zones. *Journal of Arid Environments*, *61*(3), 419–446. https://doi.org/10.1016/j.jaridenv.2004.09.025

Groeneveld, D. P., & Baugh, W. M. (2007). Correcting satellite data to detect vegetation signal for eco-hydrologic analyses. *Journal of Hydrology*, *344* (1–2), 135–145. https://doi.org/10.1016/j.jhydrol.2007.07.001

Groeneveld, D. P., Baugh, W. M., Sanderson, J. S., & Cooper, D. J. (2007). Annual groundwater evapotranspiration mapped from single satellite scenes. *Journal of Hydrology*, *344*(1–2), 146–156. https://doi.org/10.1016/j.jhydrol.2007.07.002

Huete, A. R., & Liu, H. Q. (1994). An error and sensitivity analysis of the atmospheric- and soil-correcting variants of the NDVI for the MODIS-EOS. *IEEE Transactions on Geoscience and Remote Sensing*, *32*(4), 897–905.

Jamison, L. R., Johnson, M. J., Bean, D. W., & van Riper, C. (2018). Phenology and abundance of northern tamarisk beetle, *Diorhabda carinulata* affecting defoliation of *Tamarix*. *Southwestern Entomologist*, *43*(3), 571–584. https://doi.org/10.3958/059.043.0302

Jamison, L. R., van Riper, C., & Bean, D. W. (2015). The influence of *Tamarix ramosissima* defoliation on population movements of the northern tamarisk beetle (*Diorhabda Carinulata*) within the Colorado Plateau. 281–292. doi: https://doi.org/10.2307/j.ctt183pc7f.22

Jarchow, C. J., Nagler, P. L., & Glenn, E. P. (2017). Greenup and evapotranspiration following the minute 319 pulse flow to Mexico: An analysis using Landsat 8 normalized difference vegetation index (NDVI) data. *Ecological Engineering*, *106*, 776–783. https://doi.org/10.1016/j.ecoleng.2016.08.007

Jordan, F., Jody Waugh, W., Glenn, E. P., Sam, L., Thompson, T., & Lewis Thompson, T. (2008). Natural bioremediation of a nitrate-contaminated soil-and-aquifer system in a desert environment. *Journal of Arid Environments*, *72*(5), 748–763. https://doi.org/10.1016/j.jaridenv.2007.09.002

Kennard, D., Louden, N., Gemoets, D., Ortega, S., González, E., Bean, D., … Stahlke, A. (2016). *Tamarix* dieback and vegetation patterns following release of the northern tamarisk beetle (*Diorhabda carinulata*) in western Colorado. *Biological Control*, *101*, 114–122. https://doi.org/10.1016/j.biocontrol.2016.07.004

Kerr, Y. H., Imbernon, J., Dedieu, G., Hautecoeur, O., Lagouarde, J. P., & Seguin, B. (1989). NOAA AVHRR and its uses for rainfall and evapotranspiration monitoring. *International Journal of Remote Sensing*, *10* (4–5), 847–854. https://doi.org/10.1080/01431168908903925

Liu, H. Q., & Huete, A. (1995). A feedback based modification of the NDVI to minimize canopy background and atmospheric noise. *IEEE Transactions on Geoscience and Remote Sensing*, *33*(2), 457–465.

Luttge, U., & Beyschlag, W. (2014). In J. Cushman (Ed.), *Progress in Botany* (Vol. 75). Berlin Heidelberg.

McKeon, C. A., Jordan, F. L., Glenn, E. P., Waugh, W. J., & Nelson, S. G. (2005). Rapid nitrate loss from a contaminated desert soil. *Journal of Arid Environments*, *61*(1), 119–136. https://doi.org/10.1016/j.jaridenv.2004.08.006

McKeon, C., Glenn, E. P., Waugh, W. J., Eastoe, C., Jordan, F., & Nelson, S. G. (2006). Growth and water and nitrate uptake patterns of grazed and ungrazed desert shrubs growing over a nitrate contamination plume. *Journal of Arid Environments*, *64*(1), 1–21. https://doi.org/10.1016/j.jaridenv.2005.04.008

Meng, R., Dennison, P. E., Jamison, L. R., van Riper, C., Nager, P., Hultine, K. R., … Dudley, T. (2012). Detection of tamarisk defoliation by the northern tamarisk beetle based on multitemporal Landsat 5 thematic mapper imagery. *GIScience & Remote Sensing*, *49*(4), 510–537. https://doi.org/10.2747/1548-1603.49.4.510

Nagler, P. L., Nguyen, U., Bateman, H. L., Jarchow, C. J., Glenn, E. P., Waugh, W. J., & van Riper, C. (2018). Northern tamarisk beetle (Diorhabda carinulata) and tamarisk (*Tamarix spp*.) interactions in the Colorado River basin. *Restoration Ecology*, *26*(2), 348–359. https://doi.org/10.1111/rec.12575/suppinfo

Natural Resources Conservation Service (NRCS). (n.d.). Web Soil Survey. Retrieved from https://websoilsurvey.sc.egov.usda.gov

Nichols, J., Eichinger, W., Cooper, D. I., Prueger, J. H., Hipps, L. E., Neale, C. M. U., & Bawazir, A. S. (2004). *Comparison of evaporation estimation methods for a riparian area*. Iowa City, Iowa: University of Iowa.

Reith, C. C., & Thompson, B. M. (1992). *Deserts as dumps? The disposal of hazardous materials in arid ecosystems*. Albuquerque, NM: University of New Mexico Press.

Rivers Edge West. (2018). Tamarisk Beetle Distribution Map: North American expansion of *Diorhabda* species; 2007–2018. Retrieved from https://www.arcgis.com/apps/StorytellingTextLegend/index.html?appid=937b60bde5384d32ab800ae430376d3d

Robinson, T. W. (1958). *Geological survey water-supply paper 1423*. Washington, DC: United States Geological Survey.

Sandvig, R. M., & Phillips, F. M. (2006). Ecohydrological controls on soil moisture fluxes in arid to semiarid vadose zones. *Water Resources Research*, *42*(8), 1–20. https://doi.org/10.1029/2005wr004644

Scanlon, B. R., Levitt, D. G., Reedy, R. C., Keese, K. E., & Sully, M. J. (2005). Ecological controls on water-cycle response to climate variability in deserts. *Proceedings of the National Academy of Sciences of the United States of America*, *102*(17), 6033–6038. https://doi.org/10.1073/pnas.0408571102

Sellers, P. J., Berry, J. A., Collatz, G. J., Field, C. B., & Hall, F. G. (1992). Canopy reflectance, photosynthesis, and transpiration III. A Reanalysis Using improved leaf models and a new canopy integration scheme. *Remote Sensing of Environment*, *42*, 187–216.

Tabari, H., Hosseinzadeh Talaee, P., & Some'e, B. S. (2013). Spatial modelling of reference evapotranspiration using adjusted Blaney-Criddle equation in an arid environment. *Hydrological Sciences Journal*, *58*(2), 408–420. https://doi.org/10.1080/02626667.2012.755265

Tucker, C. J., & Sellers, P. J. (1986). Satellite remote sensing of primary production. *International Journal of Remote Sensing*, *7*(11), 1395–1416. https://doi.org/10.1080/01431168608948944

Waugh, W. J., Glenn, E. P., Charley, P. H., Maxwell, B., & O'Neill, M. K. (2011). Helping mother earth heal: Diné college and enhanced natural attenuation research at U.S. Department of Energy uranium processing sites on Navajo land. In J. Burger (Ed.), *Stakeholders and scientists: Achieving implementable solutions to energy and environmental issues*. New York, NY: Springer.

Wilcox, B. P., Breshears, D. D., & Seyfried, M. S. (2003). Rangelands, water balance on. In T. A. H. B. A. Stewart (Ed.), *Encyclopedia of water science* (pp. 791–794). New York, NY: Marcel Dekker.

Winograd, I. J. (1981). Radioactive waste storage in thick unsaturated zones. *Science*, *212*, 1457–1464.

How to cite this article: Jarchow CJ, Waugh WJ, Didan K, Barreto-Muñoz A, Herrmann S, Nagler PL. Vegetation-groundwater dynamics at a former uranium mill site following invasion of a biocontrol agent: A time series analysis of Landsat normalized difference vegetation index data. *Hydrological Processes*. 2020;1–11. https://doi.org/10.1002/hyp.13772